

**Supplementary Information for**

**Solar-driven co-thermolysis of CO<sub>2</sub> and H<sub>2</sub>O and in-situ oxygen removal  
across a non-stoichiometric ceria membrane**

Maria Tou<sup>1</sup>, Jian Jin<sup>2,3</sup>, Yong Hao<sup>2,3</sup>, Aldo Steinfeld<sup>1</sup>, Ronald Michalsky<sup>1\*</sup>

<sup>1</sup> Department of Mechanical and Process Engineering, ETH Zürich, 8092 Zürich, Switzerland

<sup>2</sup> Institute of Engineering Thermophysics, Chinese Academy of Sciences, 11 Beisihuanxi Rd., Beijing 100190, P. R. China

<sup>3</sup> University of Chinese Academy of Sciences, No.19A Yuquan Rd., Beijing 100049, P. R. China

\*corresponding author

## Experimental

Membrane morphology was characterized using scanning electron microscopy (SEM). **Figure S1** shows SEM images of the inner surfaces (a, b) and cross sections (c, d) of representative ceria membranes as-prepared (a, c) and after use in the reactor for experiments with CO<sub>2</sub> and H<sub>2</sub>O (b, d). The surfaces of the membranes exhibit some inter- and intra-granular porosity. The membrane is gas-tight if pores do not connect across the thickness of the membrane, as confirmed in the cross-sectional images. The membranes were prepared with two successive coatings of the ceria slurry. The phase-inversion step after each coating resulted in two regions containing large pores in the cross section: at the edge near the outer surface and in the middle region (at the outer edge of the first coating). The grain size after use in the reactor (b) is slightly larger than in the as-prepared sample (a), suggesting further sintering and grain growth at the reaction temperature. Otherwise, the morphological structure of the membrane is generally unchanged by use in the reactor and exposure to CO<sub>2</sub> and H<sub>2</sub>O and their thermolysis products.

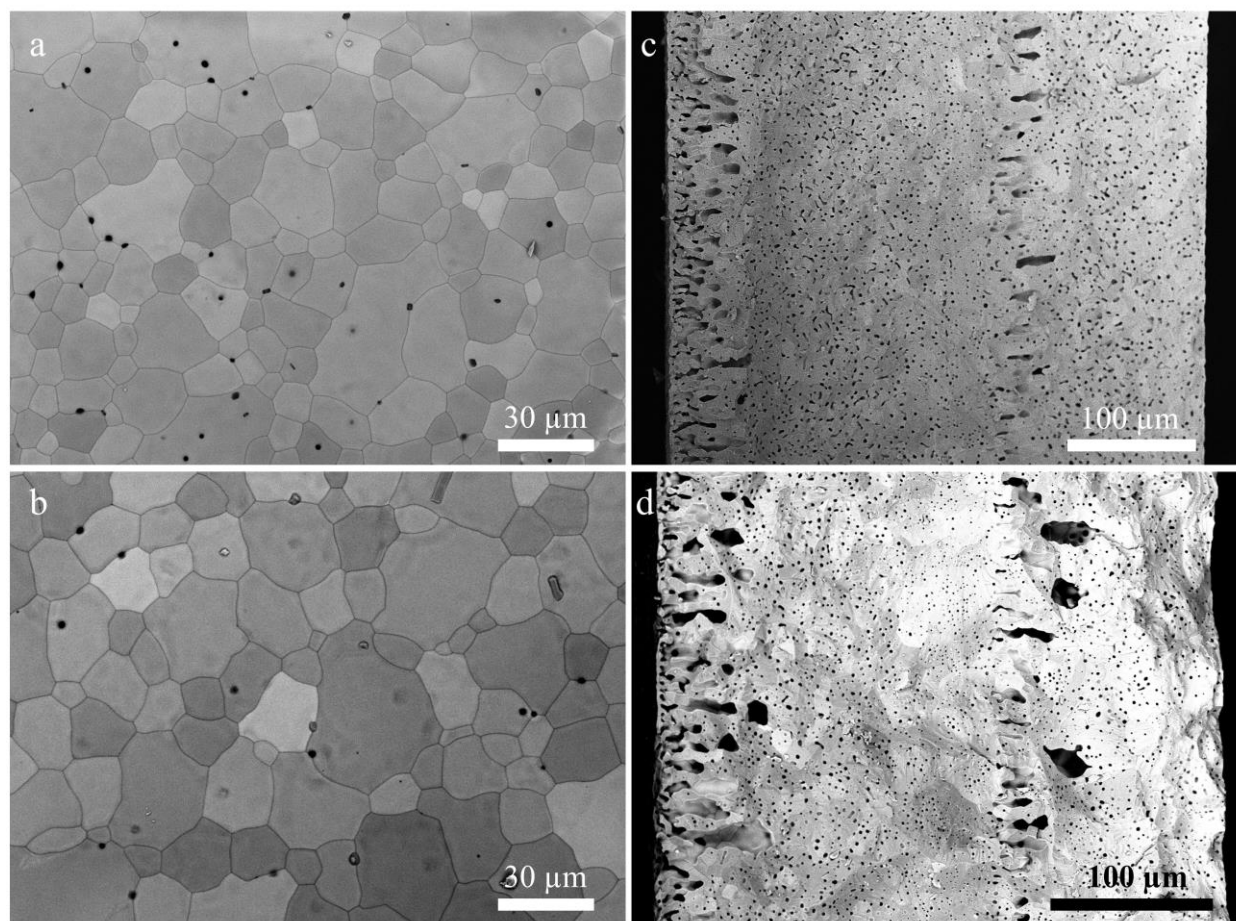


**Figure S1.** SEM images of the inner surface (a, b) and cross section (c, d) of representative ceria membranes as-prepared (a, c) and after use in thermolysis experiments with CO<sub>2</sub> and H<sub>2</sub>O (b, d).

## Thermodynamic Analysis

Ideally, temperature measurements inside the membrane would be used in the thermodynamic model for an accurate comparison with experimental results. Given the geometry of the reactor, such measurements are technically difficult and would disrupt the gas flows if done in situ. Instead, the reaction temperature inside the membrane is approximated using a simplified heat transfer model. This calculation establishes bounds on the thermodynamic limits with a rough estimate of the temperature difference between the outside of the shell tube and the inside of the membrane. Because there exist some axial measurements along the shell tube, but no additional radial measurements, axial and radial temperature gradients are considered independently.

Thermocouple measurements show that there is an axial gradient along the shell tube, and the maximum temperature is measured at the level of the cavity aperture ( $T_1$  in Figure 2). However, the membrane tube (at the temperature of interest) hangs from the top of the cavity and extends to a point above this level. At the tested conditions, the shell surface temperature measured at a level coincident with the bottom half of the membrane ( $T_2$  in Figure 2) is typically 30 K less than the maximum.

The radial gradient is approximated with a simple 1D heat transfer model, which balances the sensible heat absorbed by the gas streams and the heat of reaction with conduction through the solid tube walls and radiation between the shell and membrane tubes. As shown in **Figure S2**, the radial reactor model is divided into four regions: the solid alumina shell wall, the solid ceria membrane wall, the annular region containing the flow of sweep gas, and the cylindrical region containing the oxidant flow. The known parameters include the gas flow rates and initial  $T$ , material properties, and  $T_{\text{shell,out}}$ . For simplicity, constant material properties from the temperature range of interest are used, except for the heat capacity of  $\text{CO}_2$ , where the  $T$ -

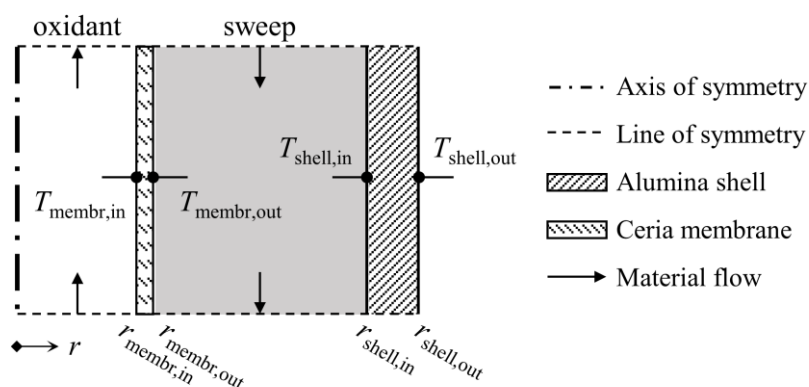


**Figure S2.** Representation of the membrane reactor as simplified for a 1D radial heat transfer model.

**Table S1.** Input parameters for simplified radial heat transfer model of the membrane reactor.

Quantity	Value	Justification
$r_{\text{shell,out}}$	12.5 mm	Experimental value
$r_{\text{shell,in}}$	10 mm	Experimental value
$r_{\text{membr,out}}$	3.5 mm	Experimental value
$r_{\text{membr,in}}$	2.5 mm	Experimental value
$L$	150 mm	Experimental value
$T_{i,\text{initial}}$	298.15 K	Ambient $T$
$T_{\text{shell,out}}$	1773-1873 K	Experimental value
$k_{\text{Al}_2\text{O}_3}$	6.3 W/(m K)	Above 1200 K <sup>1</sup>
$k_{\text{CeO}_2}$	0.837 W/(m K)	Above 1500 K <sup>1</sup>
$C_{p,\text{Ar}}$	520.64 J/(kg K)	NIST
$C_{p,\text{CO}_2}$	$f(T)$	NIST
$\chi_{\text{oxidant}}$	0.01	Experimental value
$\Delta h_{\text{rxn}}$	279 kJ/mol	1673-1873 K, NIST
$w$	0.95	Educated guess
$\varepsilon_{\text{Al}_2\text{O}_3}$	0.4	Above 1200 K <sup>1</sup>
$\varepsilon_{\text{CeO}_2}$	0.4	1800 K <sup>1</sup>

<sup>1</sup> Oxides and their solutions, in *Thermophysical properties of high temperature solid materials*, Y.S. Touloukian, Editor. The MacMillan Company: New York 1967.

dependent Shomate equation is used. A complete list of the input quantities used in the calculation is summarized in **Table S1**. It is assumed that the oxidant gas reaches thermal equilibrium with the inner wall of the membrane, thus the temperature of interest,  $T_{\text{reaction}}$ , equals  $T_{\text{membr,in}}$ . While the finite area of the tubular membrane is considered, axial effects are neglected to approximate the geometry as an infinite cylinder. Furthermore, because the feeder tube has a relatively low surface area and thermal mass, it can be neglected to simplify the geometry. The solid regions transfer heat through conduction only, whereas heat transfer across the sweep gas region is through radiation and convection. Conduction in the gas phase is neglected due to the relatively low thermal conductivity of gases. Gases are further assumed to be transparent to radiation, and thus only heated via convection. A weighted mean of the wall temperature and initial gas temperature is used to approximate a bulk temperature for the gas.

From an energy balance over the control volume from  $r = 0$  to  $r_{\text{shell,in}}$ , the heat conducted through the shell wall must equal the heat removed by both gas flows and the reaction:

$$\dot{Q}_{\text{shell,cond}} = \dot{Q}_{\text{sweep,sensible}} + \dot{Q}_{\text{oxidant,sensible}} + \dot{Q}_{\text{reaction}}, \quad (\text{S1})$$

with

$$\dot{Q}_{\text{shell,cond}} = \frac{2\pi k_{\text{Al}_2\text{O}_3} L (T_{\text{shell,out}} - T_{\text{shell,in}})}{\ln\left(\frac{r_{\text{shell,out}}}{r_{\text{shell,in}}}\right)}, \quad (\text{S2})$$

$$\dot{Q}_{i,\text{sensible}} = \dot{n}_i C_{p,i} (T_{i,\text{final}} - T_{i,\text{initial}}), \text{ and} \quad (\text{S3})$$

$$\dot{Q}_{\text{reaction}} = \chi_{\text{oxidant}} \dot{n}_{\text{oxidant}} \Delta h_{\text{rxn}}. \quad (\text{S4})$$

$\dot{Q}_{\text{shell,cond}}$  in equation (S2) is the cylindrical integrated form of Fourier's law with thermal conductivity  $k_i$  and membrane length  $L$ .  $\dot{Q}_{i,\text{sensible}}$  in equation (S3) is the sensible heat absorbed by the sweep or oxidant flow from the initial temperature,  $T_{i,\text{initial}}$ , to the final temperature at  $L$ ,  $T_{i,\text{final}}$ , given the molar flow rates and heat capacity  $C_{p,i}$ .  $\dot{Q}_{\text{reaction}}$  in equation (S4) is the heat of reaction. At the operating temperatures of the membrane reactor, radiative heat transfer is expected to dominate, and radial temperature differences will be small relative to the total temperature. Therefore, at this stage of the calculation, the final  $T$  of both gas streams is approximated by the same weighting function:

$$T_{i,\text{final}} = w T_{\text{shell,in}} + (1-w) T_{i,\text{initial}}, \quad (\text{S5})$$

where  $w$  is a weighting parameter. With this substitution, equation (S1) can be solved for  $T_{\text{shell,in}}$ .

To determine  $T_{\text{membr,out}}$ , an energy balance is formulated over the control volume from  $r = 0$  to  $r_{\text{membr,out}}$ , which equates the heat radiated to the membrane outer surface from the shell inner surface to the sum of: the heat removed by convection in the sweep gas, the sensible heat absorbed by the oxidant, and the heat of reaction,

$$\dot{Q}_{\text{shell-membr,rad}} = \dot{Q}_{\text{membr,conv}} + \dot{Q}_{\text{oxidant,sensible}} + \dot{Q}_{\text{reaction}} \quad (\text{S6})$$

with

$$\dot{Q}_{\text{shell-membr,rad}} = -\frac{A_{\text{membr,out}} \sigma (T_{\text{membr,out}}^4 - T_{\text{shell,in}}^4)}{\frac{1}{\varepsilon_{\text{CeO}_2}} + \left(\frac{A_{\text{membr,out}}}{A_{\text{shell,in}}}\right) \left(\frac{1}{\varepsilon_{\text{Al}_2\text{O}_3}} - 1\right)}, \quad (\text{S7})$$

$$\dot{Q}_{\text{membr,conv}} = h A_{\text{membr,out}} (T_{\text{membr,out}} - \bar{T}_{\text{sweep}}), \text{ and} \quad (\text{S8})$$

$$A_i = 2\pi r_i L. \quad (\text{S9})$$

Equation (S7) is obtained from the radiosity method applied to diffuse-gray concentric infinite cylinders, where  $\sigma$  is the Stefan-Boltzmann constant and  $\varepsilon_i$  is the emissivity of species  $i$ . Convective heat transfer in an enclosure is non-trivial to calculate. Instead of attempting to determine the heat transfer coefficient  $h$  and the mean bulk sweep temperature  $\bar{T}_{\text{sweep}}$  to solve equation (S8), the following relationship is used:

$$\dot{Q}_{\text{conv}} = \dot{Q}_{\text{membr,conv}} + \dot{Q}_{\text{shell,conv}} = \dot{Q}_{\text{sweep,sensible}}, \quad (\text{S10})$$

where  $\dot{Q}_{\text{conv}}$  is the total convective heat transfer in the region between the membrane and shell tubes, and  $\dot{Q}_{\text{membr,conv}}$  and  $\dot{Q}_{\text{shell,conv}}$  are the components at the membrane and shell surfaces, respectively. For the sake of solution, and because the temperatures are expected to be close, it is assumed that  $T_{\text{membr,out}} = T_{\text{shell,in}}$ . In this way,  $\dot{Q}_{\text{membr,conv}}$  can be expressed as a function of  $\dot{Q}_{\text{sweep,sensible}}$  and the relative areas of both surfaces:

$$\dot{Q}_{\text{membr,conv}} = \frac{A_{\text{membr,out}}}{A_{\text{membr,out}} + A_{\text{shell,in}}} \dot{Q}_{\text{sweep,sensible}}. \quad (\text{S11})$$

Again, the final  $T$  of both gas streams is unknown but estimated with the best available approximation using the weighting function:

$$T_{i,\text{final}} = wT_{\text{membr,out}} + (1-w)T_{i,\text{initial}}. \quad (\text{S12})$$

Then, it is possible to solve equation (S6) for  $T_{\text{membr,out}}$ .

Finally, to determine  $T_{\text{membr,in}}$ , an energy balance is formulated over the control volume from  $r = 0$  to  $r_{\text{membr,in}}$ , where the heat conducted through the membrane wall must equal the heat removed by the oxidant gas flow plus the reaction:

$$\dot{Q}_{\text{membr,cond}} = \dot{Q}_{\text{oxidant,sensible}} + \dot{Q}_{\text{reaction}}, \quad (\text{S13})$$

with

$$\dot{Q}_{\text{membr,cond}} = \frac{2\pi k_{\text{CeO}_2} L (T_{\text{membr,out}} - T_{\text{membr,in}})}{\ln\left(\frac{r_{\text{membr,out}}}{r_{\text{membr,in}}}\right)}. \quad (\text{S14})$$

Substituting equations (S3), (S4), and (S14) into equation (S13) allows evaluation of  $T_{\text{membr,in}}$ .

Following this procedure, the radial temperature difference is predicted to be about 17 K for the range of conditions tested. Because the model neglects axial gradients in the membrane, this result may underestimate the effective temperature difference. Combining the axial and radial temperature differences indicates that the maximum shell temperature is about 50 K higher than the reaction temperature inside the membrane. This value is used to calculate the lower bound of the thermodynamic limit presented in the main text.

## Results and Discussion

The experimental results from co-thermolysis of CO<sub>2</sub> and H<sub>2</sub>O can be plotted as a function of  $p_{O_2}$  in the sweep gas inlet, as shown in **Figure S3**. However, the effect of  $p_{O_2}$  on the conversion of reactants is weak in the tested range. The relative sweep rate  $\dot{n}_{\text{sweep}}/\dot{n}_{\text{oxidant}}$ , which inversely correlates with  $p_{O_2}$ , is primarily responsible for observed changes in conversion.

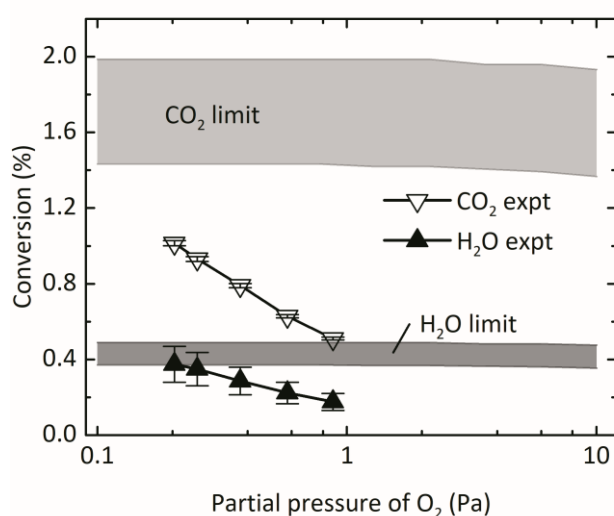


**Figure S3.** Conversion of CO<sub>2</sub> and H<sub>2</sub>O in co-thermolysis experiments as a function of  $p_{O_2}$  in the sweep gas inlet in the range 0.2 to 0.9 Pa at 1873 K. The shaded region shows the thermodynamic limit at these conditions and  $\dot{n}_{\text{sweep}}/\dot{n}_{\text{oxidant}} = 2.7$ , the average of the experimental values, which ranged from 1 to 5.